

1 Environmental thresholds in the functional mycobiome of 2 global drylands

3
4

5 Eleonora Egidi^{1,2,*}, Manuel Delgado-Baquerizo^{3,4}, Miguel Berdugo^{5,6}, Emilio
6 Guirado⁵, Davide Albanese⁷, Brajesh K. Singh^{1,2}, Claudia Coleine^{8,*}

7
8

9 ¹*Hawkesbury Institute for the Environment, Western Sydney University, Penrith, NSW,*
10 *Australia*

11 ²*Global Centre for Land-Based Innovation, Western Sydney University, Penrith, NSW,*
12 *Australia*

13 ³*Laboratorio de Biodiversidad y Funcionamiento Ecosistémico. Instituto de Recursos*
14 *Naturales y Agrobiología de Sevilla (IRNAS), CSIC, Sevilla, Spain.*

15 ⁴*Unidad Asociada CSIC-UPO (BioFun). Universidad Pablo de Olavide, Sevilla, Spain*

16 ⁵*Instituto Multidisciplinar para el Estudio del Medio “Ramon Margalef”, Universidad de*
17 *Alicante, Edificio Nuevos Institutos, San Vicente del Raspeig, Spain*

18 ⁶*Institut Department of Environmental Systems Science, ETH Zürich, Zurich, Switzerland*

19 ⁷*Research and Innovation Centre, Fondazione Edmund Mach (FEM), S. Michele all'Adige,*
20 *Italy*

21 ⁸*Department of Ecological and Biological Sciences, University of Tuscia, Viterbo, Italy*

22

23

24 Corresponding authors

25 Correspondence to Eleonora Egidi (E.Egidi@westernsydney.edu.au) and Claudia Coleine
26 (coleine@unitus.it).

27
28

29 **Abstract**

30 Fungi are major drivers of ecosystem functions. Increases in aridity are known to negatively
31 impact fungal communities in dryland ecosystems globally, however, much less is known on
32 the potential influence of other environmental drivers. To fill this knowledge gap, we
33 reanalyzed fungal data from 912 soil samples, providing the largest and most complete fungal
34 community dataset from global drylands. We used machine learning tools to examine
35 geographical patterns in community composition and spatial, edaphic, and climatic factors
36 driving them. Further, we determined critical thresholds of community turnover along those
37 gradients. Our analysis identifies UV index, climate seasonality, and sand content as the most
38 important environmental predictors of community shifts, harbouring greatest association with
39 the richness of putative plant pathogens and saprobes. Important nonlinear relationships existed
40 with each of these fungal guilds, with increases in UV and temperature seasonality above 7.5
41 and 900 SD, respectively, being associated with an increased probability of plant pathogens
42 and unspecified saprotrophs occurrence. Conversely, these environmental parameters had a
43 negative relationship with litter and soil saprotrophs richness. Consequently, these functional
44 groups might be differentially sensitive to environmental changes, which might result in an
45 inevitable disturbance of current plant-soil dynamics in drylands.

46

47

48

49

50 **Keywords:** Drylands, fungi, Fungal traits, environmental predictors, climate change,
51 thresholds

52 Introduction

53 Drylands are the largest terrestrial biome (covering about 41% of the land surface and
54 supporting 40% and 35% of the global population and global diversity, respectively) and are
55 expected to expand further up to 56% by the end of the century ¹. Drylands play key roles in
56 regulating the global carbon, nitrogen and water cycles, and are thus fundamental for sustaining
57 life on Earth ². Due to their extreme temperatures, low and variable rainfall, and low soil
58 fertility, drylands are particularly sensitive to changes in climate that lead to increased aridity
59 (i.e. precipitation/potential evapotranspiration) ³.

60 Fungi are paramount components and drive critical ecosystem services in drylands,
61 contributing to the formation of fertile islands ⁴, nutrient cycling and climate regulation ⁵, with
62 a major role in dryland primary production ⁶ and pedogenesis ⁷. Key fungal groups include
63 pathogens, mutualistic symbionts of both plants and animals, lichenized fungi, as well as soil
64 and litter saprobes. Most previous studies on the biogeography and ecological attributes of
65 fungal communities in dry systems have focussed on the role of aridity, given its role as a key
66 driver of dryland ecology ^{3,8-9}. However, other environmental factors could be potentially
67 important in predicting fungal diversity and distributions in global drylands. For example, solar
68 UV radiation is a primary driver of litter and soil organic carbon decomposition and plant
69 growth in many arid and semi-arid ecosystems ^{10,11}, suggesting a potential major contribution
70 to the occurrence of decomposers and plant-associated fungi ¹². Similarly, temperature and
71 precipitation seasonality regulate plant cover dynamics and productivity in arid systems ¹³,
72 which in turn can influence soil physical attributes important for saprotrophs, pathogen and
73 mutualists distribution, such as soil moisture, pH, structure or carbon content ^{14,15}.

74 Despite the possible centrality of multiple environmental variables in determining the spatial
75 distributions of important fungal groups, their relative contribution to fungal biogeographical
76 patterns remains largely unexplored at larger scales ¹⁶. Given the ecological and economic
77 significance of drylands, and the global role of fungi in regulating their functions, it is critical
78 to identify the environmental factors associated with distributions of fungal communities, and
79 most importantly, to test whether the dependence of fungi on those drivers are linear or non-
80 linear. The latter is important because non-linear associations between fungal distributions and
81 environmental predictors, may signal particular environmental scenarios of exacerbated
82 sensitivity (i.e., thresholds). Such abrupt shifts can mark regime shifts with potential
83 implications for ecosystem functioning, which should be monitored and managed closely if we
84 want to prevent changes of high magnitudes in the functional roles of fungi in a context of
85 climate change ¹⁷. A better understanding of the forces shaping the global biogeography of
86 dryland soil fungi can improve our ability to predict their fate under global change, and
87 therefore inform future conservation and management policies.

88 Towards this aim, we conducted a meta-analysis of multiple datasets from different dryland
89 biogeographical regions, merging sequencing data from a wide range of ecosystem and
90 climates (i.e. hot, temperate, and cold drylands) and encompassing a representative plethora of
91 all dryland sub-types (i.e. from hyper arid to dry-sub humid). We generated an unprecedented
92 database of 1,473 fungal genera from a total of 912 individual topsoil samples (top 5-10cm)
93 from all continents, including Antarctica. We examined geographical patterns in fungal
94 assemblages and the main environmental (spatial, edaphic, and climatic) factors driving them

95 as well as to establish where, along a range of environmental pressure gradients, important
96 changes in community composition occur to identify critical thresholds along those gradients.

97
98

99 **Results**

100 *General description of the dataset*

101 Our dataset represents the largest extant fungal community dataset from drylands. Compared
102 to previous large-scale studies focused on fungal diversity in drylands, our survey encompasses
103 all continents, including Antarctica, and spans all dryland subtypes (defined by their aridity
104 ranges), from hyperarid ($AI \leq 0.05$, $n = 38$), to arid ($0.05 < AI \leq 0.2$, $n = 274$), semiarid
105 ($0.2 < AI \leq 0.5$, $n = 355$), and dry sub-humid ($0.5 < AI \leq 0.65$, $n = 265$) regions of the world.
106 Samples were distributed across cold ($n = 378$), temperate ($n = 458$) and hot drylands ($n = 71$)
107 (Supplementary Information, Figure S1).

108 Of the 1,473 genera of fungi retrieved after bioinformatics analysis, 60% belonged to
109 Ascomycota, 33% to Basidiomycota and 2.6% to Glomeromycota and 2% to Zygomycota
110 (Supplementary Information, Figure S2). Out of the 66% (986) of taxa, 34.9% were saprotrophs
111 (including 11.5% wood saprotroph, 9% litter saprotrophs, and 8% soil saprotrophs), 13% plant
112 pathogens, 8% endophytic-mycorrhizal (5% ectomycorrhizal, 1% arbuscular-mycorrhizal, and
113 2% root-foliar endophytes/epiphytes), and 5% were lichenized (Supplementary Information,
114 Figure S3). Plant pathogens were mostly dominated by Dothideomycetes (37.6%) and
115 Leotiomycetes (10%), while ectomycorrhizal fungi, wood, litter and soil saprotrophs were
116 dominated by Agaricomycetes (71, 60.5, 32 and 30%, respectively) (Supplementary
117 Information, Figure S4).

118

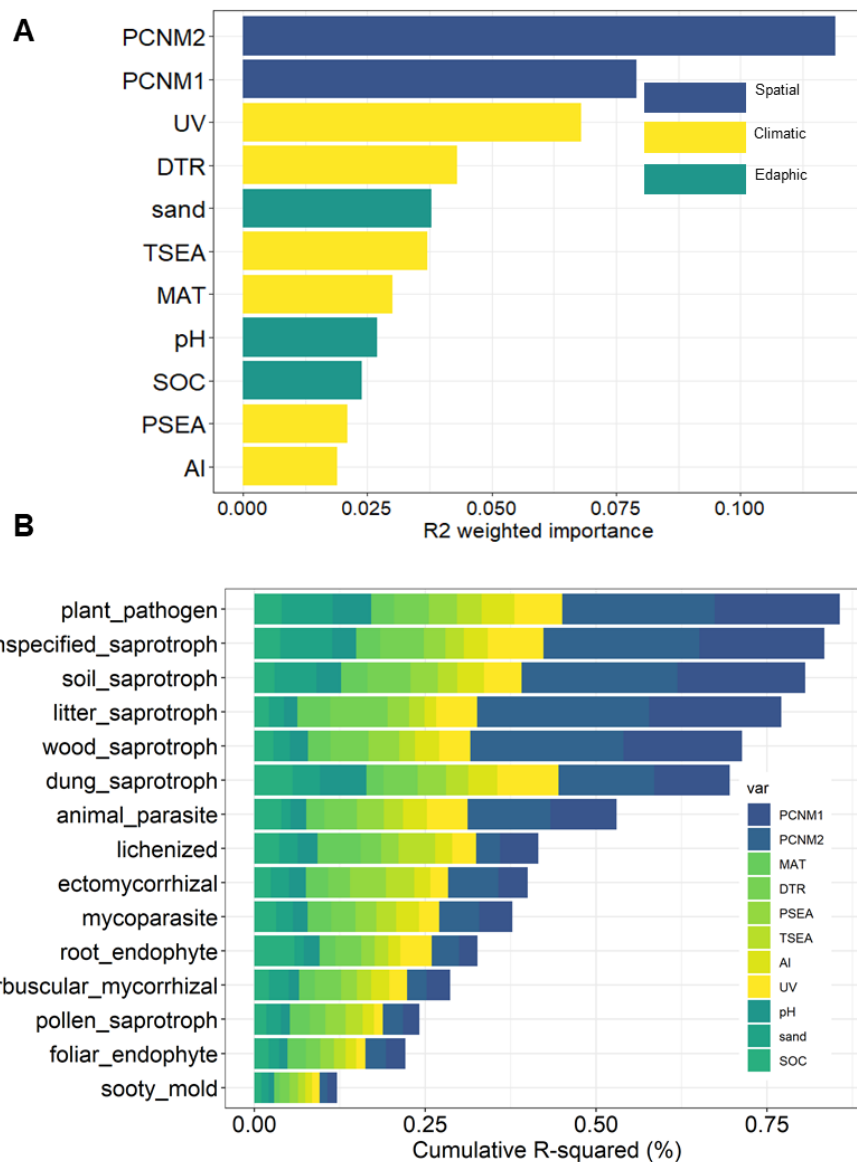
119 *Environmental drivers of functional composition*

120 The relative importance of spatial, edaphic, and climatic variables in predicting the
121 composition of the main fungal ecological groups was determined using Gradient Forest (GF)
122 methods, which identified the major determinants of community composition of fungi. The
123 total model prediction performance from the GF analysis (i.e., the proportion of variance
124 explained in a random forest) was averaged across the suite of environmental variables from
125 the most common guilds (i.e., among those occurring in at least 10% of the samples), and
126 ranged from 0.01 to 0.12 (R-squared; Figure 1A). Greatest global community turnover was
127 associated with the spatial variables (PCNM1 and PCNM1 eigenvector-based vectors,
128 maximum cumulative importance: 0.12 and 0.08, respectively), followed closely by UV index
129 (UV), with a maximum value above 0.07. Importance in relation to other environmental
130 predictors was highest (> 0.04) for diurnal temperature range (DTR), sand and temperature
131 seasonality (TSEA), while mean annual temperature (MAT), precipitation seasonality (PSEA),
132 pH, aridity index (AI) and soil organic content (SOC) had the lowest importance values (0.02-
133 0.04) (Figure 1A).

134 Then, for each ecological group, we identified the most important predictors of changes in their
135 abundance along spatial, climatic, and edaphic gradients. The cumulative model prediction
136 performance of the guilds for which significant predictive power was established (R-

137 squared >0) had a range of 0.11–0.86 (R-squared), with the highest model performance (>0.70)
138 recorded for plant pathogens and soil, litter, wood and unspecified saprotrophs (Figure 1B).
139 The predictive power of PCNM1 and PCNM2 was strongest for these fungi relative to other
140 ecological groups (R-Squared values > 0.10; Supplementary Information, Figure S5).
141 However, plant pathogen and unspecified saprotroph richness were also strongly predicted by
142 UV radiation and sand content (R-Squared values 0.07-0.08, respectively), while DTR was the
143 single most important climate predictor of litter saprotroph richness, followed by UV (R-
144 Squared values = 0.08 and 0.06, respectively). DTR was also important in predicting soil
145 saprotrophs distributions, together with sand content (R-Squared values = 0.06 for both).
146 Conversely, PSEA and TSEA were the strongest predictors of ectomycorrhizal fungi (R-
147 Squared values=0.04 and 0.05, respectively), with TSEA also strongly associating with
148 lichenised fungi (R-Squared values=0.05; Supplementary Information, Figure S5).
149

150
151
152



153
154 **Figure 1. Environmental predictors of dryland fungal community composition (A)**
155 Relative importance, R-squared (R^2), of each environmental predictor included in the gradient
156 forest analysis. **(B)** Contribution (0 to 1) of climatic, soil and spatial categories to the variation
157 explained by the complete gradient forest model for the 15 ecological groups for which
158 significant predictive power was established ($R^2 > 0$).
159
160

161

162 *Detection of thresholds*

163 Frequency histograms and density plots of the values used by the classification trees for splits
164 (i.e. the split density plots in Figure 2A) were utilised to quantify thresholds at whole
165 community scales (i.e., where important community changes occur) along the most predictive
166 environmental gradients. UV index harboured a major threshold at values > 7 , where most of
167 the data occurred (Figure 2A). This threshold corresponded to a shift in the proportion of most
168 ecological groups, including plant pathogens, litter and dung saprotrophs, as indicated by the
169 steep slope in the cumulative plots (Figure 2B). Along the two secondly most important
170 climatic variables (DTR and TSEA), we observed multiple subsequent strong splits. The fungal
171 community showed a first response with mean diurnal temperature range > 8 °C, and then a
172 second threshold with mean diurnal range > 14 °C, the latter mainly corresponding to shift in
173 proportion of a range of saprotrophic fungi (i.e. litter, soil and unspecified saprotrophs); shifts
174 in lichenized and ectomycorrhizal fungi, as well as animal and plant pathogens and dung
175 saprotrophs, was recorded with a variation of monthly temperature averages $> 1,000$ SD and $>$
176 500 SD (Figure 2A and B). Finally, important community changes related to soil edaphic
177 features were brought about by sand content between 45-60%, with shifts in plant pathogens
178 and a range of saprotrophs (unspecified, dung and soil; Figure 2A and B).

179

180
181
182

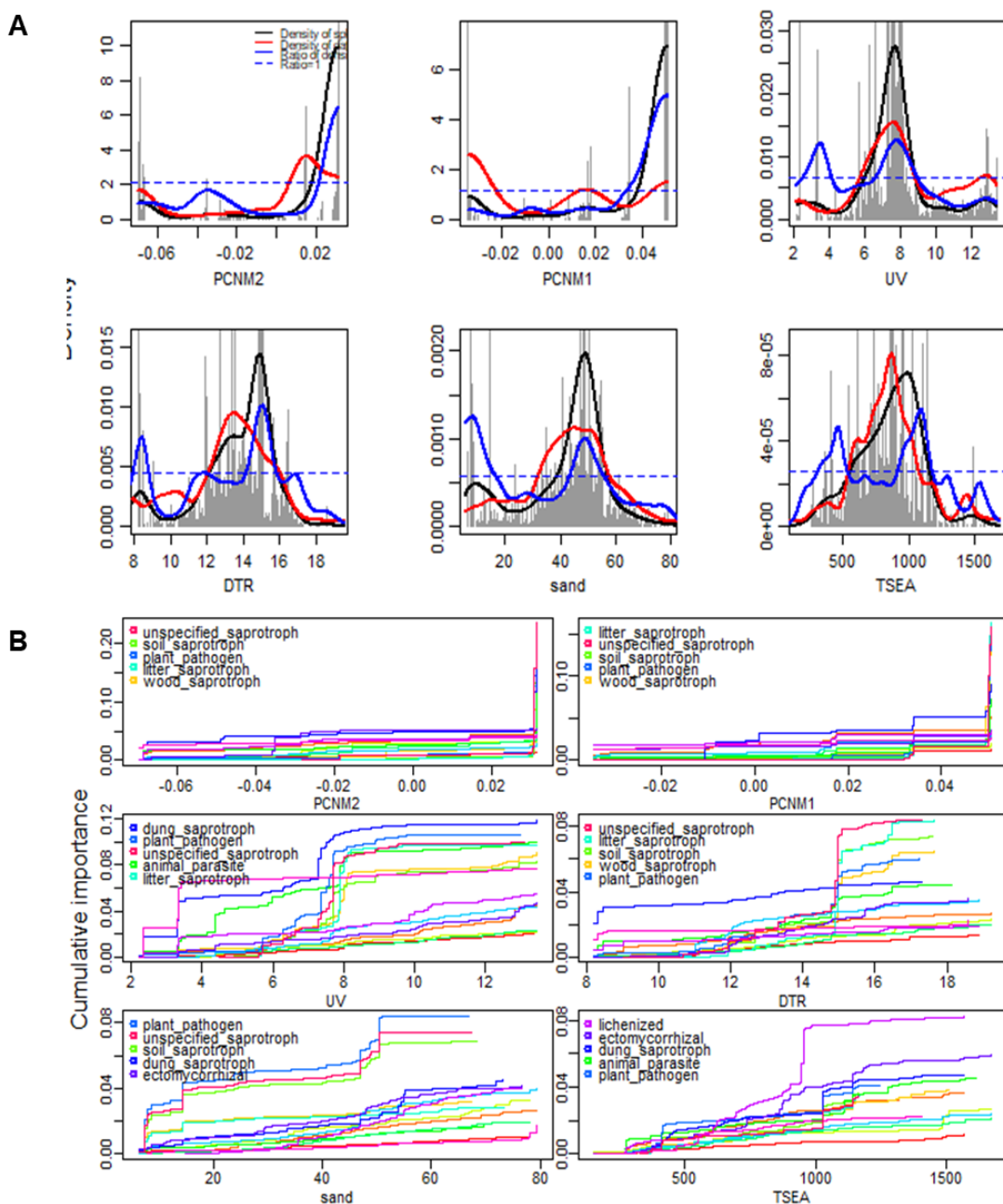


Figure 2: Most relevant predictors of fungal composition in drylands worldwide. (A)
Frequency histograms of gradient values at which splits occur in the regression trees of the top 15 ecological groups in relationship to the top six environmental variables, showing where along these gradients important compositional changes are taking place. Black lines are the kernel density of the histograms, red lines show the (normalized) distribution of the data along the environmental gradients, and blue lines indicate the ratio between splits and data (ratio between black and red lines). Ratios >1 (above the dotted line) indicate conditions of relatively greater change in genus composition (i.e. community thresholds). Individual plots depict the predictors, arranged (left to right) from the most to the least important. PSEA = precipitation seasonality; TSEA = temperature seasonality; DTR = diurnal temperature range; AI= aridity Index; UV = UV index; MAT = Mean annual temperature. **(B)** Compositional change along the top six environmental gradients for the top five fungal ecological groups. Each line denotes an

196 ecological group and their pattern of compositional change along the gradient. The y-axes
197 have been normalized so that the maximum corresponds to the relative variable importance.
198

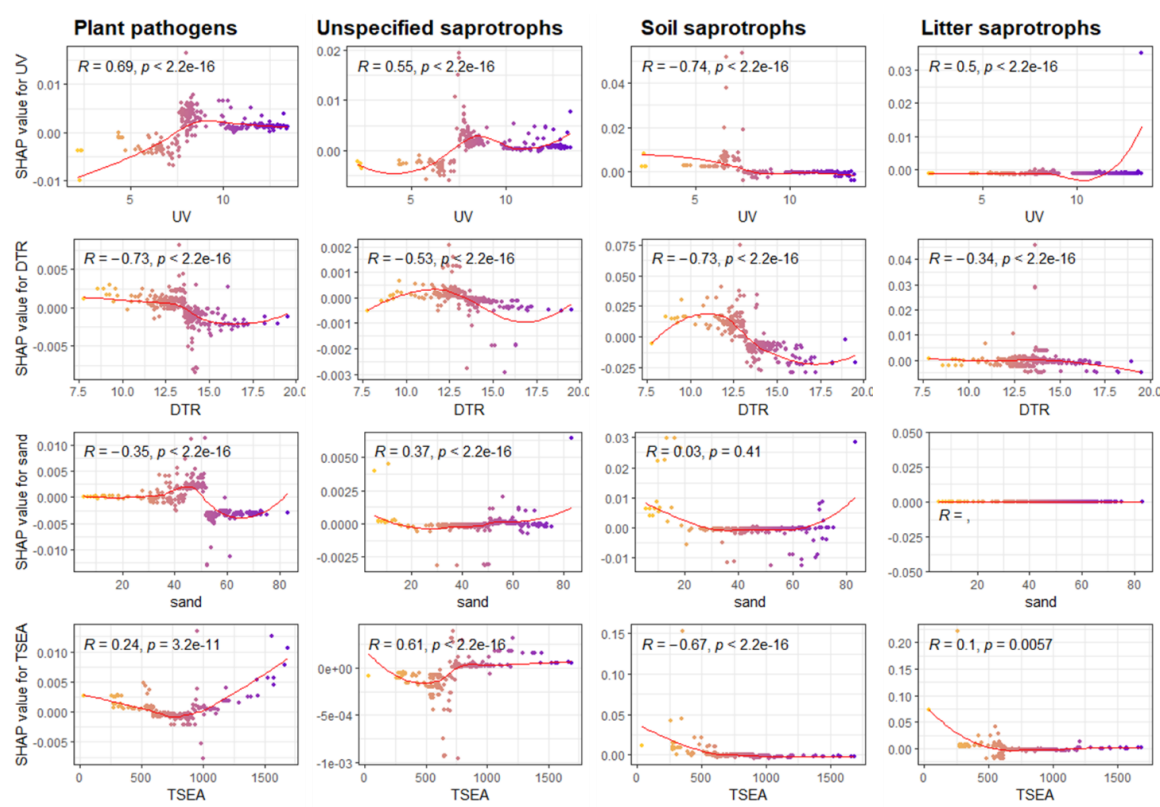
199

200 Because the results of the previous analyses do not allow to depict the relationship between
201 environmental predictors and functional guilds of fungi (they only inform about the existence
202 of a high magnitude change affecting the composition of the community), we used Random
203 Forest (RF) models for each guild and SHAP dependence plots (see Online Methods) to
204 visualise these dependencies (Figure 3). All these relationships showed different degree of non-
205 linear behaviours, with marked thresholds in the predictors signalling either abrupt (e.g.,
206 changes for DTR, sand, UV or TSEA for unspecified saprotrophs), or non-linear trends (e.g.,
207 changes occurring in TSEA) affecting probability of occurrence of fungal ecological guilds.
208 For instance, plant pathogens and unspecified saprotrophs had a higher probability of
209 occurrence with increases in UV (values > 7.5), TSEA (values > 900 SD), and decreases in
210 DTR (values < 14 °C), with pathogens also being positively associated with sand content of
211 approximately 35-50%. Soil saprotrophs were predicted to occur with decreasing UV (values
212 < 7.5), TSEA (values < 500degC), and DTR (values < 14 °C); litter saprotrophs were generally
213 most likely to occur at narrower TSEA (values < 500 SD).

214

215

216



217

218 **Figure 3: Distribution and environmental predictors of the main fungal ecological**
219 **groups in drylands.** Shapley additive explanations (SHAP) dependence plot of selected
220 climatic and edaphic predictors of plant pathogens and saprotrophs richness in drylands. The
221 effect is expressed as SHAP values, which measure the impact of each predictor on the model
222 output (richness of a particular fungal ecological group). SHAP values are derived for a given
223 predictor value in a process analogous to partial dependence plots; thus each point on the
224 plot corresponds to a prediction in a sample (see methods).

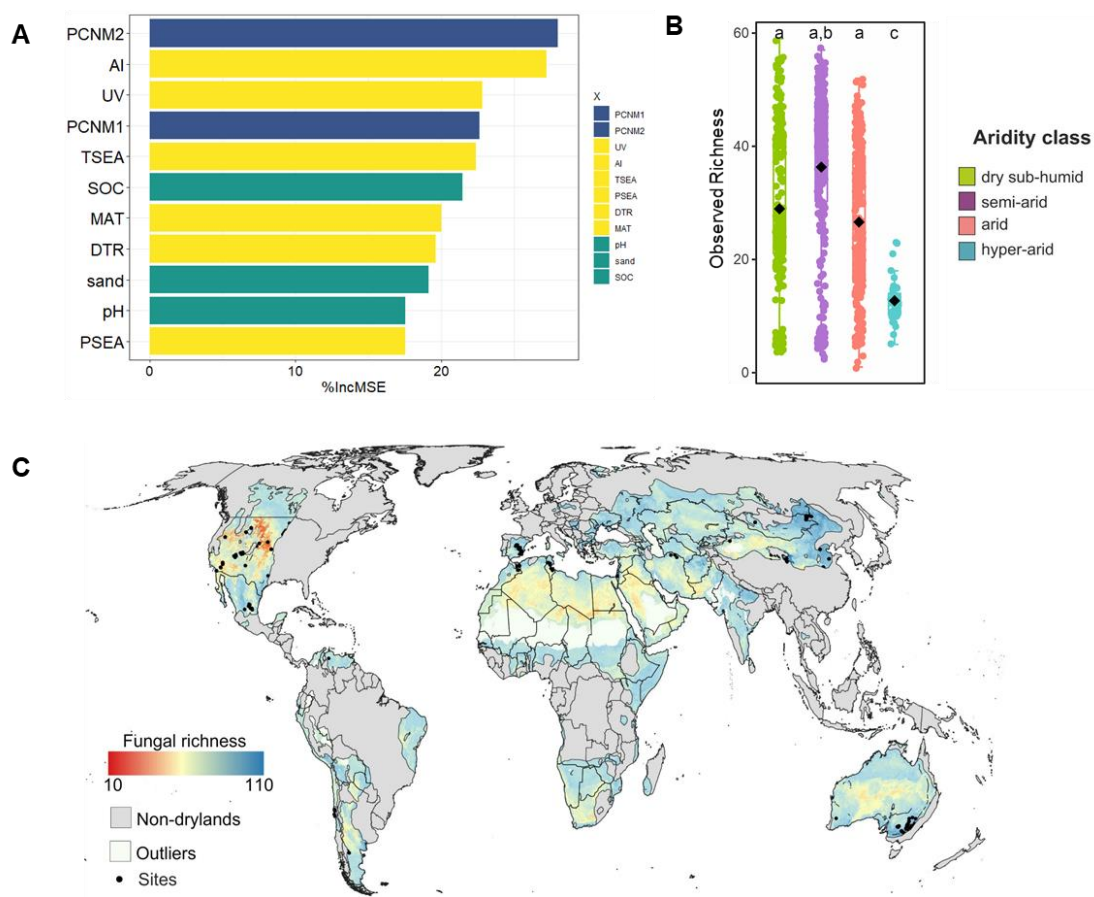
225 R = Spearman Rho correlation coefficient; p = p value.

226

227 *Global patterns of fungal diversity in drylands*

228 The Random Forest model built to assess the relative contribution of environmental predictions
229 of overall fungal richness in drylands revealed a strong contribution of spatial distance
230 (PCNM1) and AI (%IncMSE > 20 for both; Figure 4A). We observed generally similar levels
231 of richness between dry sub-humid, semi-arid and arid biomes, while hyper-arid areas
232 supported a significantly lower (Wilcoxon test, $p > 0.05$) fungal diversity (Figure 4B).
233 Consistently, the fungal maps estimating the expected geographical distribution and richness
234 of dryland fungi ($R=0.92$, Figure 4C), broadly reflected the extent of well-characterised high
235 classes of aridity, with sharp declines in fungal alpha diversity in hyper-arid regions of the
236 globe.

237



238
239

240 **Figure 4. Environmental predictors of dryland fungal community richness.** (A) Relative
241 importance, expressed as %IncMSE, of each environmental predictor included in the random
242 forest analysis. (B) Box-plots illustrating alpha diversity indices (Observed richness) of fungal
243 phylotypes (genus level) for the different aridity classes. Individual data points, median values
244 and interquartile ranges are shown. Different letters indicate significant differences ($P < 0.05$,
245 Wilcoxon test). (C) Predicted global distribution of fungal richness across drylands worldwide.
246 The scale bar represents the observed richness of each ecological group.

247
248

249 Discussion

250 Our study demonstrates, for the first time, that environmental gradients related with solar UV
251 radiation (i.e., the UV index), climate seasonality (i.e., DTR and TSEA) and soil structure (i.e.,
252 sand content) are critical predictors of fungal community composition in global dryland soils,
253 with the greatest influence detected in association with the richness of putative plant pathogens
254 and a range of fungal saprotrophic groups. Most importantly, we found that the relationships
255 of these environmental predictors with different fungal ecological groups are markedly non-
256 lineal, exhibiting thresholds in the values of environmental variables that may signal
257 particularly vulnerable environmental scenarios. In particular, increases in UV and temperature
258 seasonality above a certain threshold (7.5 and 900 SD, respectively) were associated with an
259 increased probability of plant pathogens and unspecified saprotrophs occurrence, with plant
260 pathogens also being positively associated with sand content of approximately 35-50%.
261 Conversely, these parameters had an overall negative relationship with litter and soil
262 saprotrophs richness, the latter being negatively influenced also by increases in DTR (values >
263 14 °C).

264 These trends can be explained by the unique abiotic features that regulate biogeochemical
265 cycling in drylands and the peculiar physiological attributes of different saprotrophic and
266 pathogenic fungal groups ¹⁸. In most arid lands, temperature-related variables and soil structure
267 are considered critical factors in determining decomposers composition ¹⁹, and traditional
268 models identify extreme temperatures and low soil moisture typical of dry regions of the world
269 as main controllers of litter quality and microbial activities ²⁰. These environmental parameters
270 can thus act as limiting factors for the distribution of fungal decomposer, which tend withstand
271 overall lower temperature ranges compared to other guilds, such as pathogenic fungi ²⁸, thus
272 explaining their decrease in occurrence probability with increases in temperature ranges and
273 variability ¹⁵. Soil structure attributes are also expected to exert various influences on fungal
274 communities, for example by enhancing substrate availability from SOC pools, while also
275 controlling water holding capacity ²¹, which can in turn regulate fungal saprotroph richness and
276 composition.

277 Similarly, in many arid ecosystems, solar radiation is considered a primary driver of
278 decomposition and carbon cycling ²²²³, resulting in a significant photo priming effect that
279 controls root exudation, litter quality and nutrient availability, and accelerates abiotic-driven
280 decomposition in these systems ²⁴. The tight link between UV radiation and biogeochemical
281 cycling in drylands could thus explain the prominent role of the UV index in predicting the
282 distributions of saprotrophic groups associated with soil and litter, and the overall negative
283 influence on soil saprotroph richness.

284 Conversely, putative plant pathogens were mostly dominated by ascomycetes from the classes
285 Dothideomycetes and Leotiomycetes, which are known to possess unique physiological traits
286 allowing them to resist environmental stresses typical of drylands, including UV radiation, high
287 temperature fluctuations and dissection ^{7,9,25}. Such common traits might allow potential
288 pathogens from these taxonomic groups to adapt to a wide range of environmental stressors,
289 possibly explaining the ability of the members of this ecological group to thrive in extreme
290 environments. Additionally, photoreception and light-dependent traits have been recently
291 suggested as a likely mechanism allowing foliar pathogens from sun-lit habitats to recognize

292 potential partners and stressed hosts²⁶, indicating that increases in UV radiation might have an
293 important but underestimated role in facilitating the establishment of pathotrophic fungi in
294 dryland ecosystems. Our analyses indicate that countries crossing a 7.5 UV radiation index
295 threshold and experiencing high temperature seasonality (values > 900 SD) could be at
296 increased risk of pathogen outbreaks, with potentially detrimental ecological and economic
297 implications.

298 Overall, the relative importance of the environmental predictors identified in our survey is
299 markedly different from the findings from previous global studies conducted in more mesic
300 environments, where mean annual precipitation has the strongest influence on the richness of
301 most fungal taxonomic and functional guilds^{27,28}, reflecting the peculiarity of the
302 environmental attributes that regulate ecosystem functionality in drylands. Interestingly, the
303 aridity index, which is considered a primary driver of change in drylands³, had a secondary
304 role in determining fungal functional changes in our dataset. However, in line with other global
305 surveys, we observed significant decline in fungal alpha diversity with increasing aridity,
306 confirming the critical role of this climatic variable in shaping microbial biodiversity in global
307 drylands. The compositional turnover of the dryland functional mycobiome was also strongly
308 associated with the eigenvector-based spatial descriptors (PCNMs), which were also
309 significantly correlated to the total fungal community richness. At the guild level, the strongest
310 effect was recorded for phototrophic and saprotrophic fungi, the most abundant members of
311 the community in our dataset. The large predictive power of PCNMs could indicate a role for
312 neutral processes, such as dispersion limitation and/or stochastic events, in shaping the
313 community dynamics of the dominant fraction of the fungal assemblies²⁹. Indeed, abundant
314 microbial taxa with higher dispersal rates tend to be affected by drift or priority effects more
315 than their rarer counterparts³⁰, possibly explaining the large influence of spatial variables
316 observed in this study for the most frequent functional groups. However, the overall
317 performance of our models remained relatively low for the less common functional guilds in
318 the dataset, suggesting that other processes such as biotic interactions³¹, or unmeasured
319 environmental gradients (e.g., vegetation composition^{32,33}) might play a critical role in
320 characterising the distribution of these lower abundance community members in dry
321 ecosystems, and warrant further investigations on a global scale.

322 Collectively, our results indicate that solar UV radiation, temperature and precipitation
323 variability, and soil structure might be underappreciated drivers of global distribution of
324 critically important fungal groups, such as plant pathogens and saprobes. The relationships
325 between functional composition and environment uncovered in this study are crucial for
326 developing accurate mechanistic models and making predictions about climate-driven shifts in
327 fungal community structure, and thus ecosystem functions. Overall, our findings imply that
328 processes leading to shifts in solar radiation (e.g., stratospheric ozone depletion), soil structure
329 (e.g., land-use change, and land degradation), and seasonal climatic patterns (e.g., increases in
330 atmospheric levels of a greenhouse gases), might have disproportionate consequences for the
331 distribution of fungal groups linked to vegetation and biogeochemical cycling in drylands, and
332 could influence the balance of plant–soil interactions in drylands. These processes might be
333 particularly exacerbated in the Southern Hemisphere, where climate change has profound
334 influence on the ozone layer³⁴, and could be further compounded by predicted increases in
335 extreme heatwave events, which can synergistically alter the UV-mediated effects on terrestrial

336 ecosystems^{35,36}. In particular, we observed a significant threshold in composition turnover at
337 UV index > 7 and diurnal temperature ranges > 900 SD, suggesting that the strongest effects
338 of climate-driven shifts in UV incidence and climate seasonality could occur in regions
339 approaching these values, such as arid regions of the Australia, Centre and South America,
340 North Africa and Central Asia³⁷, with unknown ecosystem-level implications.

341 Taken together, the comprehensive catalogue of ecology–climate relationships we provide
342 paves the way to a more exhaustive and detailed understanding of the complex role of climate
343 and soil in regulating fungal biogeography, especially in those regions of the world that are
344 most vulnerable to environmental changes, such as global drylands. This work opens a new
345 line of investigation to include quantifying the importance of abiotic and biotic processes that
346 govern fungal communities across contrasting regions of the world, with particular emphasis
347 on identifying the traits, and traits trade-offs, underpinning their functional capabilities in such
348 unique ecosystems³⁸. In particular, we anticipate that as strain-specific trait data become
349 available, better assessment of functional variation expressed within and among communities
350 in relation to UV tolerance and climate variability will be possible. This information is required
351 to provide better predictions of the current and future adaptation of fungi to the effects of
352 climate change, and their ramifications for sustainability of dryland ecosystems.

353

354

355 **Online Methods**

356 *Literature and environmental variables selection*

357 We have undertaken a comprehensive meta-study of data published on the composition of soil
358 fungal communities in drylands across the world. This approach enabled us to re-analyse
359 multiple datasets from different biogeographical regions and biomes and compile a large
360 dataset of fungal taxa distribution worldwide (see Supplementary Material for details on
361 literature selection, bioinformatics data processing, and functional group assignments). In total,
362 14 studies, encompassing over 912 top-soil (5–10 cm depth) sampling points, were identified
363 and included in the analysis; this allowed us to encompass all continents (including Antarctica;
364 Supporting Information Figure S1), spanning a wide range of environmental conditions. The
365 final sample list included all drylands subtypes (hyper-arid, AI 0.0–0.05, n = 42; arid, AI =
366 0.05–0.20, n = 274; semiarid, AI = 0.20–0.50; n = 336; dry-sub humid, AI = 0.50–0.65; n =
367 264).

368 Metadata were collected from the published papers and/or public repositories where they were
369 submitted by the authors, while in a few cases from the authors of individual studies upon
370 request and are included in Supporting Information. Additional metadata were collected from
371 the Worldclim database (<https://www.worldclim.org>; ~1 km resolution)³⁹, and included
372 spatial, climatic and edaphic parameters. Climatic data included a range of variables related to
373 temperature and precipitation variability that are considered important drivers of fungal
374 distribution at large scales²⁸ – i.e., mean annual temperature (MAT), precipitation seasonality
375 (PSEA), temperature seasonality (TSEA) – as well as the aridity index (AI). The aridity index
376 was obtained from the global maps of⁴⁰, which provides the averaged AI of the period 1970–
377 2000, and has a spatial resolution of 30 arc-seconds. We also collected data on the AI from the
378 Global Potential Evapotranspiration database⁴¹, which is based on interpolations provided by

379 WorldClim. We used aridity index instead of mean annual precipitation in our study because
380 aridity includes both mean annual precipitation and potential evapotranspiration, and is
381 therefore a more accurate metric of the long-term water availability at each site; moreover
382 aridity index is the one used for categorizing drylands and is the one used on global reports
383 about desertification and climate change. UV radiation (UV) was further included given its
384 importance in driving biogeochemical processes in dryland soils^{18,41}. Three important edaphic
385 determinants of fungal biogeography (i.e., % of sand, SOC and pH), obtained from SoilGrids
386 v2 database, were also included, allowing us to evaluate the importance of soil physico-
387 chemical attributes for fungal distribution in drylands. To accommodate spatial variables,
388 principal coordinates of neighbour matrices (PCNMs) were also included as explanatory
389 variables in downstream analyses to examine the importance of spatial filters on community
390 composition⁴². PCNMs were calculated with the vegan R package, and the first two of the
391 positive PCNMs were retained. We obtained complete environmental metadata for a total of
392 743 samples, which were used for the quantification of the functional turnover across
393 environmental gradients (see methods below). Downstream analysis, unless otherwise
394 specified, were performed in R environment v. 4 and using the genus-level taxonomy table.
395

396 *Quantification of ecological turnover and thresholds across environmental gradients*

397 To explore the environmental drivers of distributions of the most common fungal ecological
398 guilds in global drylands, we modelled their occurrence using an approach similar to⁴³. Briefly,
399 we first identified the most common guilds among those occurring in at least 10% of the
400 samples, which resulted in 16 ecological groups. We then explored the most important
401 environmental predictors of fungal ecological turnover by generating a random forest fitting a
402 total of 500 trees using the extended modelling procedure available in R package
403 “gradientForest”⁴⁴. The gradient forest (GF) technique derives monotonic, nonlinear functions
404 that characterize compositional shifts along each fitted environmental gradient, without a priori
405 distributional assumptions about the frequency of response variables, as opposed to other
406 methods such as generalized linear models or generalized additive models. The importance of
407 each predictor variable (measured as R-squared) in the model is assessed by quantifying the
408 decrease in performance when each predictor variable is randomly permuted, using a
409 conditional approach which accounts for collinearity between predictor variables⁴⁵. This
410 allows us to assess each predictor's importance relative to one another in terms of their
411 influence on patterns of composition. Additionally, GF allows the development of empirical
412 distributions that represent species (ecological groups in this case) turnover along each
413 environmental gradient, by aggregating the values of the tree splits from the Random Forest
414 models for all individual models with positive fits (R-squared > 0). The turnover function is
415 measured in dimensionless R-squared units where groups with highly predictive random forest
416 models (i.e., high R-squared values) have greater influence on the turnover functions than those
417 with low predictive power (i.e., lower R-squared). These turnover functions can provide unique
418 insights into the nature of how functional patterns vary along multiple environmental gradients,
419 at the level of individual ecological groups as well as the mycobiome as a whole when these
420 individual curves are averaged to obtain a global R-squared value. The incremental approach

421 to model fitting in GF makes it also well suited for the analysis of large datasets, whose size
422 can be limiting in other approaches, such as generalized dissimilarity modelling⁴⁶. A detailed
423 description of these methods can be found in^{44,47}.

424 Following the GF approach described above, the model performance was assessed by the
425 overall goodness-of-fit (R-squared) of predicted against observed values and by the cross-
426 validated out-of-bag R-squared values per ecological group, while the significance of each
427 environmental variable was assessed by the relative importance weighted by R-squared values
428⁴⁴. Subsequently, to visualize the importance and abruptness of specific thresholds and to
429 identify common threshold locations among ecological groups, we plotted their cumulative
430 importance, whereby the shape of the resulting distribution curves describes the magnitude of
431 compositional change along the most important gradients, with the standardized ratio of split
432 density >1 indicating the highest manifestation of a threshold⁴⁸. The concept of community
433 threshold used here is defined as a zone along an environmental gradient where the change in
434 community composition is enhanced as a result of sharp increases or decreases in the
435 occurrence of several functional groups (depending on the direction of the gradient). Therefore,
436 GF enabled us to identify critical values along environmental gradients that correspond to
437 threshold changes in functional composition.

438 Finally, to further illustrate the directionality of the response to environmental predictors, we
439 run GradientBoost (GB) models with SHapley Additive exPlanations (SHAP) dependence
440 plots. GB models were run individually for each ecological group and were done solely for the
441 most important environmental variables and ecological groups best explained by the GF
442 models. The SHAP method is derived from game theory and measures how much each feature
443 of a model contributes to the increase or decrease of the probability of a single output with
444 respect to the average of the ones used to train the model (ie, the richness of a particular
445 ecological group in this case). In a nutshell, the SHAP value is derived from a regression tree
446 model for a given feature and prediction. Its value is the effect of the predictor of interest in
447 the model output for a given prediction and, thus it is provided in the same units as the response
448 variable. SHAP values are actually homologous to evaluating the expression $\beta_1 * x_1$ in a regular
449 multiple regression ($y \sim \beta_1 * x_1 + \beta_2 * x_2 + \dots + \beta_n * x_n$). This means that, essentially, a given
450 predicted value of the model is the summation of all SHAP values obtained from the model
451 given the values of predictors (74). By plotting the values of predictor vs the associated SHAP
452 values we obtain a response curve analogous to the effects of that predictor over the response
453 variable (i.e., a partial dependence plot). SHAP values are widely used in machine learning
454 (75), economics (72), security (73) and ecology (76). SHAP values can be positive or negative,
455 whereby a positive trend indicates that a feature is expected to positively influence the
456 occurrence of a particular ecological group, and vice-versa. Models were built with the
457 “xgboost” package and SHAP values were extracted with the “SHAPforxgboost” package in
458 R.

459
460

461 *Quantification of biodiversity and environmental drivers of fungal community
462 composition*

463 Alpha diversity was estimated using the R package ‘phyloseq’⁴⁹, calculating biodiversity

464 indices as the species richness as a count of the observed taxa in each sample. A Random Forest
465 (RF) model was built using the ‘randomForest package with 500 trees in R to assess the relative
466 contribution of climatic, spatial and edaphic predictors on dryland fungal richness. Statistical
467 analysis was performed to identify how overall richness changed across dryland types by one-
468 way analysis of variance (one-way ANOVA) and pairwise multiple comparison procedure
469 (Tukey test); a small probability p-value (<0.05) indicated a significant difference. The extent
470 of the global distribution of soil fungal richness was estimated using a Random Forest
471 regression analysis as described in the supplementary material.

472 **Data availability**

473 Metadata and samples ID are freely available in Figshare
474 (<https://doi.org/10.6084/m9.figshare.19243749.v1>)

475 **Code availability**

476 The codes for the computational analyses are available in Figshare
477 (<https://doi.org/10.6084/m9.figshare.19243749.v1>).

478

479 **Acknowledgements**

480 C.C. acknowledge funding from the Italian National Program for Antarctic Research (PNRA)
481 and is supported by a PNRA postdoctoral fellowship. E.E. is supported by an Australian
482 Research Council DECRA fellowship (DE210101822). M.D-B. is supported by a project from
483 the Spanish Ministry of Science and Innovation (PID2020-115813RA-I00), and a project
484 PAIDI 2020 from the Junta de Andalucía (P20_00879). Microbial distribution and colonization
485 research in B.K.S.’s lab is funded by the Australian Research Council (DP190103714). E.G. is
486 supported by the European Research Council Grant agreement 647038 (BIODESERT).

487

488 **Authors' contributions**

489 E.E. and C.C. developed the original idea of the analyses presented in the manuscript.
490 Literature selection and raw data retrieving were done by C.C. Bioinformatic analyses were
491 done by D.A and C.C.. Statistical analyses, environmental modelling and data interpretations
492 were done by E.E., M.B., E.G., M.D-B., and C.C. The manuscript was written by E.E. with
493 contributions from all the co-authors. All authors have read and agreed to the published version
494 of the manuscript.

495 **Competing interests**

496 The authors declare no competing interests.

497

498 **References**

499 1. Cherlet, M. *et al. World Atlas of Desertification: Rethinking Land Degradation and*
500 *Sustainable Land Management.* (2018).

501 2. Maestre, F. T. *et al.* Biogeography of global drylands. *New Phytol.* **231**, 540–558 (2021).

502 3. Berdugo, M. *et al.* Global ecosystem thresholds driven by aridity. *Science* **367**, 787–790 (2020).

503 4. Cherlet, M. *et al.* *World Atlas of Desertification: Rethinking Land Degradation and Sustainable Land Management.* (2018).

504 5. Delgado-Baquerizo, M. *et al.* Soil microbial communities drive the resistance of ecosystem multifunctionality to global change in drylands across the globe. *Ecol. Lett.* **20**, 1295–1305 (2017).

505 6. Rudgers, J. A. *et al.* Are fungal networks key to dryland primary production? *Am. J. Bot.* **105**, 1783–1787 (2018).

506 7. Coleine, C., Stajich, J. E., de Los Ríos, A. & Selbmann, L. Beyond the extremes: Rocks as ultimate refuge for fungi in drylands. *Mycologia* **113**, 108–133 (2021).

507 8. Maestre, F. T. *et al.* Increasing aridity reduces soil microbial diversity and abundance in global drylands. *Proc. Natl. Acad. Sci. U. S. A.* **112**, 15684–15689 (2015).

508 9. Egidi, E. *et al.* A few Ascomycota taxa dominate soil fungal communities worldwide. *Nat. Commun.* **10**, 2369 (2019).

509 10. Bornman, J. F. *et al.* Solar ultraviolet radiation and ozone depletion-driven climate change: effects on terrestrial ecosystems. *Photochem. Photobiol. Sci.* **14**, 88–107 (2015).

510 11. Zepp, R. G., Erickson, D. J., 3rd, Paul, N. D. & Sulzberger, B. Interactive effects of solar UV radiation and climate change on biogeochemical cycling. *Photochem. Photobiol. Sci.* **6**, 286–300 (2007).

511 12. Paul, N. D. & Gwynn-Jones, D. Ecological roles of solar UV radiation: towards an integrated approach. *Trends Ecol. Evol.* **18**, 48–55 (2003).

512 13. Palmquist, K. A. *et al.* Divergent climate change effects on widespread dryland plant communities driven by climatic and ecohydrological gradients. *Glob. Chang. Biol.* **27**, 5169–5185 (2021).

513 14. Egidi, E. *et al.* Delving into the dark ecology: A continent-wide assessment of patterns of composition in soil fungal communities from Australian tussock grasslands. *Fungal Ecol.* **39**, 356–370 (2019).

514 15. Feng, Y. *et al.* Temperature thresholds drive the global distribution of soil fungal decomposers. *Glob. Chang. Biol.* (2022) doi:10.1111/gcb.16096.

515 16. Osborne, P., Hall, L. J., Kronfeld-Schor, N., Thybert, D. & Haerty, W. A rather dry subject; investigating the study of arid-associated microbial communities. *Environ Microbiome* **15**, 20 (2020).

516 17. Pausas, J. G. & Bond, W. J. On the Three Major Recycling Pathways in Terrestrial Ecosystems. *Trends Ecol. Evol.* **35**, 767–775 (2020).

517 18. Throop, H. L. & Archer, S. R. Resolving the dryland decomposition conundrum: Some new perspectives on potential drivers. in *Progress in Botany* 171–194 (Springer Berlin Heidelberg, 2008).

518 19. Zhu, B. & Cheng, W. Constant and diurnally-varying temperature regimes lead to different temperature sensitivities of soil organic carbon decomposition. *Soil Biol. Biochem.* **43**, 866–869 (2011).

519 20. A'Bear, A. D., Jones, T. H., Kandeler, E. & Boddy, L. Interactive effects of temperature and soil moisture on fungal-mediated wood decomposition and extracellular enzyme

activity. *Soil Biol. Biochem.* **70**, 151–158 (2014).

21. Hu, Y. *et al.* Soil organic carbon and soil structure are driving microbial abundance and community composition across the arid and semi-arid grasslands in northern China. *Soil Biol. Biochem.* **77**, 51–57 (2014).

22. Bornman, J. F. *et al.* Solar ultraviolet radiation and ozone depletion-driven climate change: effects on terrestrial ecosystems. *Photochem. Photobiol. Sci.* **14**, 88–107 (2015).

23. Brandt, L. A., King, J. Y., Hobbie, S. E., Milchunas, D. G. & Sinsabaugh, R. L. The role of photodegradation in surface litter decomposition across a grassland ecosystem precipitation gradient. *Ecosystems* **13**, 765–781 (2010).

24. Day, T. A., Bliss, M. S., Tomes, A. R., Ruhland, C. T. & Guénon, R. Desert leaf litter decay: Coupling of microbial respiration, water-soluble fractions and photodegradation. *Glob. Chang. Biol.* **24**, 5454–5470 (2018).

25. Gostinčar, C., Muggia, L. & Grube, M. Polyextremotolerant black fungi: oligotrophism, adaptive potential, and a link to lichen symbioses. *Front. Microbiol.* **3**, 390 (2012).

26. Schumacher, J. & Gorbushina, A. A. Light sensing in plant- and rock-associated black fungi. *Fungal Biol.* **124**, 407–417 (2020).

27. Tedersoo, L. *et al.* Fungal biogeography. Global diversity and geography of soil fungi. *Science* **346**, 1256688 (2014).

28. Větrovský, T. *et al.* A meta-analysis of global fungal distribution reveals climate-driven patterns. *Nat. Commun.* **10**, 5142 (2019).

29. Dumbrell, A. J., Nelson, M., Helgason, T., Dytham, C. & Fitter, A. H. Relative roles of niche and neutral processes in structuring a soil microbial community. *ISME J.* **4**, 337–345 (2010).

30. Mo, Y. *et al.* Biogeographic patterns of abundant and rare bacterioplankton in three subtropical bays resulting from selective and neutral processes. *ISME J.* **12**, 2198–2210 (2018).

31. Bahram, M. *et al.* Stochastic distribution of small soil eukaryotes resulting from high dispersal and drift in a local environment. *ISME J.* **10**, 885–896 (2016).

32. Hiiesalu, I., Bahram, M. & Tedersoo, L. Plant species richness and productivity determine the diversity of soil fungal guilds in temperate coniferous forest and bog habitats. *Mol. Ecol.* **26**, 4846–4858 (2017).

33. Davison, J. *et al.* Temperature and pH define the realised niche space of arbuscular mycorrhizal fungi. *New Phytol.* **231**, 763–776 (2021).

34. Barnes, P. W. *et al.* Ozone depletion, ultraviolet radiation, climate change and prospects for a sustainable future. *Nat. Sustain.* **2**, 569–579 (2019).

35. Brandt, L. A., King, J. Y. & Milchunas, D. G. Effects of ultraviolet radiation on litter decomposition depend on precipitation and litter chemistry in a shortgrass steppe ecosystem. *Glob. Chang. Biol.* **13**, 2193–2205 (2007).

36. Vidović, M. *et al.* Ultraviolet-B component of sunlight stimulates photosynthesis and flavonoid accumulation in variegated *Plectranthus coleoides* leaves depending on background light. *Plant Cell Environ.* **38**, 968–979 (2015).

37. Noce, S., Caporaso, L. & Santini, M. A new global dataset of bioclimatic indicators. *Sci. Data* **7**, 398 (2020).

38. Zanne, A. E. *et al.* Finding fungal ecological strategies: Is recycling an option? *Fungal*

589 589 *Ecol.* **46**, 100902 (2020).

590 590 39. Fick, S. E. & Hijmans, R. J. WorldClim 2: new 1-km spatial resolution climate surfaces
591 for global land areas. *Int. J. Climatol.* **37**, 4302–4315 (2017).

592 592 40. Zomer, R. J., Trabucco, A., Bossio, D. A. & Verchot, L. V. Climate change mitigation: A
593 spatial analysis of global land suitability for clean development mechanism afforestation
594 and reforestation. *Agric. Ecosyst. Environ.* **126**, 67–80 (2008).

595 595 41. Trabucco, A. & Zomer, R. Global Aridity Index and Potential Evapotranspiration (ET0)
596 Climate Database v2. (2019) doi:10.6084/m9.figshare.7504448.v3.

597 597 42. Borcard, D., Gillet, F. & Legendre, P. Spatial Analysis of Ecological Data. *Use R!* 299–
598 367 (2018) doi:10.1007/978-3-319-71404-2_7.

599 599 43. Chen, K. & Olden, J. D. Threshold responses of riverine fish communities to land use
600 conversion across regions of the world. *Glob. Chang. Biol.* **26**, 4952–4965 (2020).

601 601 44. Ellis, N., Smith, S. J. & Roland Pitcher, C. Gradient forests: calculating importance
602 gradients on physical predictors. *Ecology* vol. 93 156–168 (2012).

603 603 45. Ellis, N., Smith, S. J. & Roland Pitcher, C. Gradient forests: calculating importance
604 gradients on physical predictors. *Ecology* vol. 93 156–168 (2012).

605 605 46. Stephenson, F. *et al.* Using Gradient Forests to summarize patterns in species turnover
606 across large spatial scales and inform conservation planning. *Divers. Distrib.* **24**, 1641–
607 1656 (2018).

608 608 47. Baker, M. R. & Hollowed, A. B. Delineating ecological regions in marine systems:
609 Integrating physical structure and community composition to inform spatial management
610 in the eastern Bering Sea. *Deep Sea Res. Part 2 Top. Stud. Oceanogr.* **109**, 215–240
611 (2014).

612 612 48. Roland Pitcher, C. *et al.* Exploring the role of environmental variables in shaping patterns
613 of seabed biodiversity composition in regional-scale ecosystems. *J. Appl. Ecol.* **49**, 670–
614 679 (2012).

615 615 49. McMurdie, P. J. & Holmes, S. phyloseq: an R package for reproducible interactive
616 analysis and graphics of microbiome census data. *PLoS One* **8**, e61217 (2013).